Chemical Physics Letters 612 (2014) 214–218

Contents lists available at ScienceDirect

Chemical Physics Letters

journal homepage: www.elsevier.com/locate/cplett

Thermodynamic characterization of two layers of CO_2 on a graphite surface

T.T. Trinh[a], D. Bedeaux[a], J.-M. Simon[b], S. Kjelstrup[a,c,*]

[a] Department of Chemistry, Norwegian University of Science and Technology, Trondheim, Norway
[b] Laboratoire Interdisciplinaire Carnot de Bourgogne, UMR-6303 CNRS-Université de Bourgogne, Dijon, France
[c] Department of Process and Energy Laboratory, Delft University of Technology, Delft, The Netherlands

ARTICLE INFO

Article history:
Received 3 July 2014
In final form 8 August 2014
Available online 14 August 2014

ABSTRACT

We find by examination of density profiles that carbon dioxide adsorbs on graphite in two distinct layers. We report the activity coefficient, entropy and enthalpy for CO_2 in each layer using a convenient computational method, the Small System Method, thereby extending this method to surfaces. This opens up the possibility to study thermodynamic properties for a wide range of surface phenomena.

1. Introduction

Phase transformations [1], formations of nanostructures [1,2], metastable phases [3] or agglomerations [4], as well as chemical reactions [5] are all phenomena which become special at surfaces. A surface can also pose a major barrier to transport [6,7]. Thermodynamic data will improve the understanding and dynamic modeling of equilibrium and nonequilibrium states. But thermodynamic data for surfaces are not easily available by experiments. With the introduction of the Small System Method [8,9] computational results have become feasible. This method has so far not been used to study surfaces. In this work we extend the method to a technically important process, the physisorption of CO_2 on a graphite surface. Graphitic membranes are promising cheap candidate membranes for CO_2 separation purposes [10]. The process can be written:

$$CO_2(g) + \text{graphite} \leftrightharpoons CO_2(s) \tag{1}$$

where (g) means gas phase and (s) means adsorbed gas. The purpose of the work is to demonstrate how thermodynamic information can be gained of an adsorbed state using the new simulation method. We shall see that adsorption takes place in two distinct thermodynamic layers, and that the filling into the layers can be regarded as a trade-off between the entropies and enthalpies found for each layer.

2. Methods

The Small System Method [8,9] makes use of the relation between the inverse of thermodynamic correction factor and the fluctuation in particle number N. For a surface, the relation is

$$\frac{1}{\Gamma} = \left[\frac{\langle N^2\rangle - \langle N\rangle^2}{\langle N\rangle}\right]_{T,\mu,A} \tag{2}$$

Fluctuations are sampled in small open systems (disks) with area A inside a reservoir. The reservoir is created as a large rectangular box with periodic boundary conditions. The temperature, T, and the chemical potential, μ, in the reservoir are controlled. The thickness of the sampling system is set to the thickness of the surface (see below). The area of the sampling system is varied, varying the radius of the disk, L. The smallest radius used is so small that it allows only one molecule inside the disk; the largest radius contains 20–30 molecules. The inverse thermodynamic factor is a linear function of the $1/L$ [11–13] in a particular range, to be found for each case:

$$\frac{1}{\Gamma} = \frac{1}{\Gamma^{\infty,s}}\left[1 + \frac{B}{L}\right] \tag{3}$$

Here B is a small system specific constant and superscript ∞ means the value in the thermodynamic limit. By extrapolating the linear regime to the thermodynamic limit, we obtain the wanted quantity $\Gamma^{\infty,s}$. Later on we use $\Gamma^s = \Gamma^{\infty,s}$ for simplicity.

The chemical potential of a gas adsorbed to a surface in a layer i is:

$$\mu_i^s = \mu_i^{0,s} + RT\ln a_i^s = \mu_i^{0,s} + RT\ln \gamma_i^s \frac{C_i^s}{C_i^{0,s}} \tag{4}$$

* Corresponding author at: Department of Chemistry, Norwegian University of Science and Technology, Trondheim, Norway.
E-mail addresses: trinhthanhthuat@gmail.com (T.T. Trinh), signe.kjelstrup@ntnu.no (S. Kjelstrup).

http://dx.doi.org/10.1016/j.cplett.2014.08.026

Here $\mu_i^{0,s}$ is the standard chemical potential, a^s is the (dimensionless) activity of the adsorbed phase, C^s is the surface excess concentration, and γ^s is the activity coefficient. The standard state is the hypothetical ideal state having $\gamma^s = 1$ at layer saturation, $C^{0,s}$ (given in particles per (nm^2)). The entropy follows from the standard relation $S^s = -(d\mu^s/dT)$ and the enthalpy of the layer from $H_i^s = \mu_i^s + TS_i^s$. We shall find these properties for the adsorption (1). Total surface excess concentrations (adsorptions) are defined according to Gibbs [14,15]

$$C^s = \int_0^\infty (C(z) - C^g(\alpha)\theta(z-\alpha))\, dz \tag{5}$$

where $C(z)$ and C^g are the concentrations of adsorbed molecules and of molecules in the gas phase, respectively. The integration is carried out from the equimolar surface of graphite (at $z = 0$) to the bulk gas phase ($z = \infty$). The Heaviside function, θ, is by definition unity when the argument is positive, and zero when the argument is negative. For definition of layer concentrations, see Section 3. The thermodynamic factor is also defined by:

$$\Gamma^s = 1 + \left(\frac{\partial \ln \gamma^s}{\partial \ln C^s}\right)_{T,A} \tag{6}$$

We can determine the activity coefficient by integrating Eq. (6) from zero adsorption, once the thermodynamic factor is known from the Small System Method. This gives

$$\int_1^{\gamma^s} d\ln \gamma^s = \int_0^{C^s} (\Gamma^s - 1) d\ln C^s \tag{7}$$

When $C^s \to 0$, there is no interaction between particles, meaning that $\gamma^s = 1$. We also have

$$\mu^s - \mu^{s\prime} = \int_{\mu^{s\prime}}^{\mu^s} d\mu^s = RT \int_{C^{s\prime}}^{C^s} \Gamma^s d\ln C^s \tag{8}$$

meaning that we can find the chemical potential at any adsorption relative to a reference state (indicated by $'$) from this equation. We shall use this relation to determine the standard state chemical potential $\mu_i^{0,s}$ by plotting the left hand side of Eq. (8) versus $\ln(\gamma_i^s C_i^s / C_i^{0,s})$, extrapolating to the state where this expression is zero.

3. Simulation details

The system consisted of sheets of graphite and CO_2 molecules. The graphite was made from 5 sheets of graphene without any defects. We oriented the sheets in the box such that the sheet surfaces were perpendicular to the z-axis. The distance from the graphite surface was measured along this axis, taking the equimolar surface of graphite as zero. The graphite layers were fixed in space, still yielding good results for adsorption and diffusion of gas on the surface [16,17]. A rigid body model, TraPPE, was used for CO_2 [18]. The intermolecular potential between CO_2–CO_2 was a shifted and truncated 12-6 Lennard–Jones (LJ) potential [19] with long-range Coulomb interactions, which were dealt with using the Ewald summation technique [19]. The interaction between CO_2 and the C-atoms of graphite was similarly described by a LJ potential. Details of parameters for the simulation were given earlier [16]. They have been confirmed to yield an accurate adsorption energy for CO_2 on graphite surface [16].

Classical molecular dynamics (MD) simulations were performed using the LAMMPS package [20]. A snapshot of the system is given in Figure 1, showing graphite at 500 K with CO_2 in a relatively dense gas and in an adsorbed state. Periodic boundary conditions were used for the reservoir in all directions. The simulation was done with time steps of 0.001 ps. The initial configuration was constructed by randomly distributing CO_2 molecules above the graphite surface. The system was stabilized during 2000 ps by runs with constant $N_{tot}V_{tot}T$ using Nosé–Hoover thermostats [21].

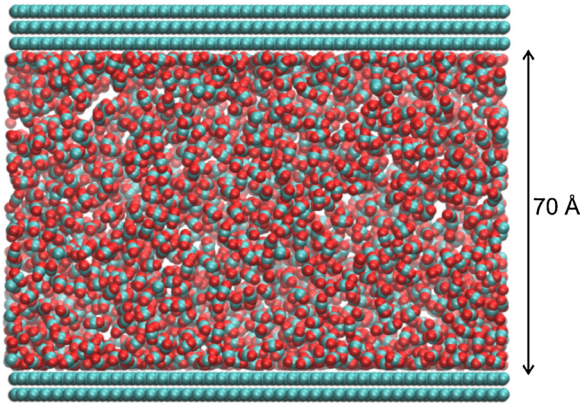

Fig. 1. Snapshot showing CO_2 in the gas phase at a fluid-like density and adsorbed on a graphite surface at 500 K. The number of CO_2 particles in the system was N_{CO_2} = 2800. The green and red colors represent carbon and oxygen atoms, respectively. (For interpretation of the references to color in this figure legend, the reader is referred to the web version of this article.)

In order to check the range of validity of Eq. (3), the reservoir size was varied. The reservoir has to be large enough compared to the sampling system. For a hard sphere system, we found that a suitable reservoir had a length 20 times the hard sphere radius L [12,13]. Simulation box sizes of (a = 42 Å, b = 54 Å, c = 84 Å), (2a, 2b, c), and (3a, 3b, c) were tested. The largest systems gave identical results, so box (2a, 2b, c) was used.

We performed 2000 ps runs in a reservoir at thermal equilibrium, varying L from 1.3 to 20 Å, sampling randomly 30 disks across the graphite surface. The total number of frames was 10 000. Hence, the value of Γ^s for each L was obtained from the statistics of 300 000 samples [11,13]. The sampling was done for temperatures ranging from 300 K to 550 K, and for a number of CO_2 particles in the box, varying from 200 to 2800 (corresponding to a pressure range of 1–60 bar at 300 K).

4. Results and discussion

4.1. Adsorptions

We describe first how we find the adsorptions C_1^s and C_2^s for each layer. The total adsorption is then $C^s = C_1^s + C_2^s$. The adsorption (excess concentration) of CO_2 was found using the results in Figure 2 with the definition (5). The figure shows the density of CO_2 molecules as a function of the distance to the graphite surface, and is a quantification of snapshots like the one showed in Figure 1. We observe in both figures that CO_2 can form two layers on the graphitic surface. In Figure 2, we see a layer around the first peak which extends from the graphite surface to position α, while a second peak extends from α to β. We refer to the integral in Eq. (5) due to the first peak as the bottom layer adsorption, while the corresponding integral related to the second peak, is called the top layer adsorption on the graphite. The position of the first peak at 5 Å covers approximately one molecular layer, as the length of the molecule is 5.4 Å. The snapshot shows that most of the carbon dioxide molecules are lying parallel to the surface. This gives a height more like the diameter of an oxygen ion, 3.6 Å. A thickness of 5 Å can be interpreted to include some molecules which are standing slightly tilted with respect to the surface, and such molecules can also be found by visual inspection of Figure 1. It is interesting that the position of plane α is always near 5 Å, independent of the temperature. This can reflect that molecules are either lying or standing

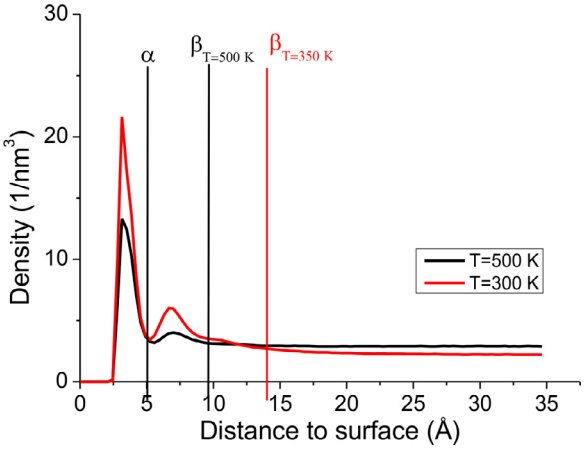

Fig. 2. The density of CO_2 molecules as a function of distance to the surface in a reservoir with $N_{CO_2} = 2800$. The temperatures are 500 K and 350 K. We distinguish between three zones, from 0 to α: first adsorbed layer, α to β: top adsorbed layer, above β: gas phase. The bottom layer extends to around 5 Å. The thickness of the top layer is larger at 350 K than that at 500 K.

in the first layer. The attractive forces of the graphite, not being able to reach above the layer, seem to be central for this layer. But the fact that the top layer starts to be filled before the bottom layer is full, motivates a division of the whole surface into two layers. The top layer, which extends from α to β, appears also rather different from the first. We see from Figure 2 that the position of the plane β varies with temperature, unlike the position of plane α. For the system with 2800 CO_2 molecules, β is smaller at 500 K than at 350 K. The top layer is thus more diffuse. Few attractive forces are able to keep the molecules within this surface layer, when the molecular kinetic energy becomes larger. The adsorption of CO_2 on graphite is always higher at low temperature in both layers, meaning that this kind of trade-off between kinetic and potential energies applies to both layers.

We find that the bottom layer has always more than half of the total adsorption, independent of temperature (not shown). The fraction is larger, the lower the temperature is, but does not exceed 0.9. The fraction decreases with increasing total adsorption, because the bottom layer becomes saturated, while the top layer keeps growing. Full coverage (maximum adsorption) of the bottom layer is obtained at 300 K with $C_1^{0,s} = 12.5\,(\text{molecules/nm}^2)$. We therefore chose as standard state, the ideal state with $C_1^{0,s} = 12.5\,(\text{molecules/nm}^2)$, corresponding to 0.31 CO_2 molecule per surface carbon atom.

4.2. The thermodynamic correction factor

Results for the inverse thermodynamic factor $(\Gamma^s)^{-1}$ were plotted versus $1/L$ for the top and bottom layers separate and for their combination (not shown). The curves approached unity as expected, when $1/L$ was increased. This is the small system limit, which has at most one particle in the sampling system. In order to find the thermodynamic limit value, we applied linear regression to points in the interval $0.1 < 1/L < 0.4$ and extrapolated the line to large L. The region used for extrapolation coincided with the region found earlier [11,13].

The thermodynamic limit value of the inverse thermodynamic correction factor $(\Gamma^s)^{-1}$ was plotted as a function of the adsorption in each single layer, and in the combined layers, for all temperatures. A typical example is shown in Figure 3 for $T = 500$ K. The bottom layer had always the smallest $(\Gamma^s)^{-1}$, while the total layer had the biggest value of $(\Gamma^s)^{-1}$. We found that $(\Gamma^s)^{-1}$ decreased more or less linearly with the adsorption. The results for the

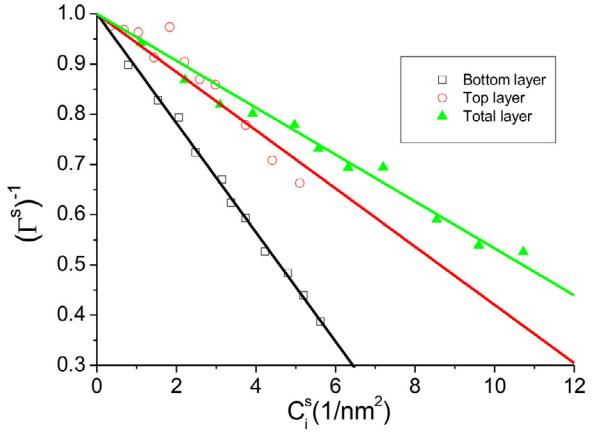

Fig. 3. Thermodynamic limit values for $(\Gamma^s)^{-1}$ in the top, bottom and total CO_2 layer on graphite at 500 K. A straight line is fitted to the results and forced through 1 on the y-axis.

bottom layer and the two layers combined (the total layer) followed the straight line nicely, while the scatter of results around the line drawn for the top layer was larger.

All curves must extrapolate to a thermodynamic correction factor equal 1, when the adsorption goes to zero. This was found the relation between $(\Gamma^s)^{-1}$ of the total layer and the total adsorption was quite linear. The observed linear dependencies mean that the inverse thermodynamic factor of the total layer, can be found by adding contributions from the bottom and top layers.

4.3. The activity coefficients for carbon dioxide in the surfaces

A set of typical activity coefficients, obtained at 500 K from Eq. (7), are shown in Figure 4. The coefficients approach 1 as expected at low density, some with more noise than others. The increase in the coefficient for the bottom layer is larger than for the top layer and therefore larger than for the total layer. This reflects that the molecules are further apart in the top layer than in the first, making repulsive forces less relevant in the top than in the bottom layer. The molecules do not adsorb, unless the surface binding energy can overcome the repulsion, however. The total layer activity coefficient was expressed as a function of total surface adsorption at different temperatures, with a regression coefficient 0.99 or better:

$$\gamma_i^s = 1 + aC_i^s + b(C_i^s)^2 \tag{9}$$

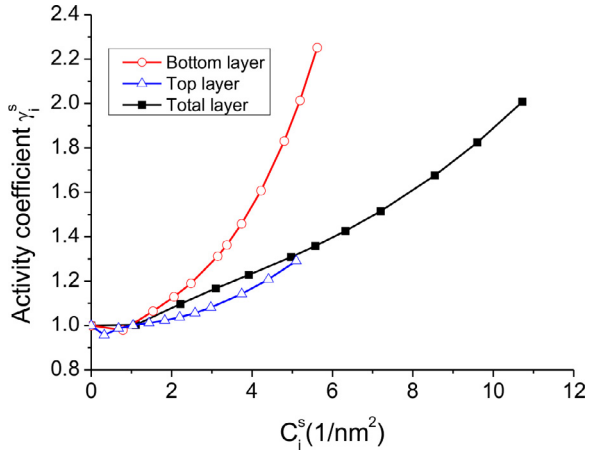

Fig. 4. Activity coefficient of bottom, top and total layer as a function of the layer adsorption in the respective layer at $T = 500$ K.

Table 1
Parameters that describe the total layer activity coefficient in the empirical Eq. (9). The regression coefficient was 0.99 or better.

T(K)	b	a
300	0.0060	0.0005
350	0.0059	0.0054
400	0.0055	0.0066
450	0.0059	0.0233
500	0.0057	0.0320
550	0.0067	0.0216

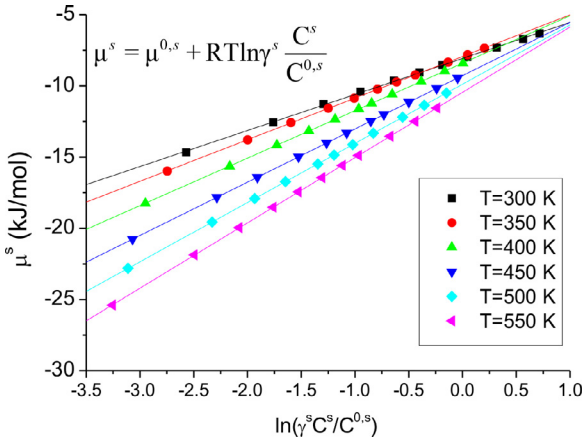

Fig. 5. Chemical potential of CO_2 on a graphite surface as a function of $\ln(\gamma^s C^s/C^{0,s})$ at different temperatures. The straight line is fitted to Eq. (4).

Parameters a and b are given in Table 1. These results may be useful for thermodynamic modeling of the total CO_2 adsorbed on a graphite surface (Fig. 5).

4.4. The chemical potential of the surface adsorbed gas

The chemical potential of the adsorbed state relative to the chemical potential at the lowest adsorption was found from Eq. (8). The chemical potential difference for the total layer was plotted vs the right hand side for the different temperatures used. Using the relevant activity coefficient and $C_1^{0,s} = C_2^{0,s} = C^{0,s} = 12.5$ molecules/(nm^2), we next used Eq. (4) to plot the same data. The slope of the linear fit gave RT as expected with good accuracy. The standard state value, $\mu^{0,s}$, was found for each temperature from this curve setting $\ln \gamma_i^s(C_i^s/C_i^{0,s}) = 0$. For the total layer, we obtained $\mu^{0,s}(T^0) = -7.6$ kJ/mol at 298 K. The temperature variation of the chemical potential was used to find the standard entropy $S^{0,s} = 10.6$ J(mol K). It was constant in the temperature interval used. The standard enthalpy at 298 K was then calculated to $H^{0,s} = -4.4$ kJ/mol. Data for the total and separate layers are given in Table 2.

In order to check that the results for the separate layers were internally consistent, we expressed the chemical potentials of the top and bottom layers of CO_2 by Eq. (2). At equilibrium, we have $\mu_1^s = \mu_2^s$, where the subscript denotes layer number. By introducing expression (2) into this equilibrium condition, we obtained

$$\left(\frac{C_1^s}{C_2^s}\right) = \left(\frac{\gamma_2^s}{\gamma_1^s}\right) e^{(\mu_2^{0,s} - \mu_1^{0,s})/RT} \tag{10}$$

By plotting the left hand side versus the ratio of activity coefficients, fitting the plot to a straight line, we calculated $\mu_2^{0,s} - \mu_1^{0,s}$ from the slope as a function of temperature. The difference in the standard chemical potentials was consistent with the difference obtained from the data in Table 2.

The thermodynamic data that we have determined for the total layer of adsorbed gas, are reasonable. The standard chemical potential and the enthalpy are both negative, indicating that adsorption is favorable in the standard state, in spite of a large reduction in the entropy from the gas phase to the surface, a reduction which is larger than that from the gas to the liquid state. We have furthermore seen that we can distinguish between two separate thermodynamically defined layers of carbon dioxide within the whole layer on the graphite surface. Each layer has its own thermodynamic properties. We see from Table 2, that the bottom layer entropy is relatively small compared to the gas entropy of CO_2. In fact it can compare to the carbon entropy in a graphite lattice. The negative entropy difference represented by the ordering of CO_2 when it is adsorbed must be overcome by a relatively large enthalpy for adsorption into the layer. The top layer entropy is larger than the entropy of the bottom layer. It is not gas-like, but four times higher than that of the bottom layer value. This layer can therefore be stabilized with a smaller enthalpy. The total layer properties can be said to mask the properties of the single layers, as the total layer has standard entropy closer to the top layer, and an enthalpy more like the bottom layer. Information of the separate layers obtained from the simulation will therefore add insight to the system. Such insight cannot be easily obtained by experiments, as it is difficult to distinguish between the layers in an adsorption experiment. It is however rather simple to compare an experimentally obtained adsorption isotherm to the adsorption isotherm derived here for the total adsorption.

5. Conclusion

We have shown that a recently developed Small System Method can be used to calculate a consistent set of thermodynamic data for surfaces from one Molecular Dynamics simulation. For carbon dioxide adsorbed to graphite, we determined the chemical potential, the activity coefficient, the entropy and enthalpy directly. Closer inspection of density profiles revealed that we can speak of two, not one layer of adsorbed gas. The thermodynamic analyses reveal a distinction between the layers. The gas has larger entropy in the top than in the bottom layer, is more mobile in this layer. The two layers are in equilibrium with one another, meaning that a lowering of the entropy can take place, if the enthalpy can compensate for the change in entropy when a top particle moves to the bottom layer. Such information is invaluable in the modeling and explanation of surface processes. Extensions to other surfaces should be straightforward.

Table 2
Thermodynamic data for standard state adsorption of carbon dioxide at a graphite surface at $T = 298$ K. The uncertainty in the determinations is on the average 3%. Corresponding values for graphite and carbon dioxide gas are also given.

$T = 298$ K	Total layer (this work)	Bottom layer (this work)	Top layer (this work)	Graphite[a]	CO_2 gas[a]
$\mu_i^{0,s}$ (kJ/mol)	−7.6	−9.8	−5.1	–	–
$S_i^{0,s}$ (J/mol K)	10.6	4.1	13.7	5.74	213.78
$H_i^{0,s}$ (kJ/mol)	−4.4	−8.6	−1.0	1.05	9.36

[a] Values from Ref. [22].

Acknowledgments

The authors acknowledge The Research Council of Norway RCN project no 209337 and The Faculty of Natural Science and Technology, Norwegian University of Science and Technology (NTNU) for financial support. The calculation power is granted by The Norwegian Metacenter for Computational Science (NOTUR). ETH Zürich is thanked for guest professorships to SK and DB.

References

[1] L.P.H. Jeurgens, Z.M. Wang, E.J. Mittemeijer, Int. J. Mater. Res. 100 (2009) 1281.
[2] F. Costache, S. Kouteva-Arguirova, J. Reif, Appl. Phys. A 79 (2004) 1429.
[3] R. Bradley Shumbera, H.H. Kan, J.F. Weaver, Surf. Sci. 601 (2007) 235.
[4] D.J. Srolovitz, M.G. Goldiner, JOM: J. Min. Met. Mater. Soc. 47 (1995) 31.
[5] M.P. Cox, G. Ertl, R. Imbihl, J. Rustig, Surf. Sci. 134 (1983) L517.
[6] I. Inzoli, J.M. Simon, S. Kjelstrup, Langmuir 25 (2009) 1518.
[7] I. Inzoli, J.M. Simon, D. Bedeaux, S. Kjelstrup, J. Phys. Chem. B 112 (2008) 14937.
[8] X. Liu, S.K. Schnell, J.M. Simon, D. Bedeaux, S. Kjelstrup, A. Bardow, T.J. Vlugt, J. Phys. Chem. B 115 (2011) 12921.
[9] P. Krüger, S.K. Schnell, D. Bedeaux, S. Kjelstrup, T.J. Vlugt, J.-M. Simon, J. Phys. Chem. Lett. 4 (2012) 235.
[10] X. He, J. Arvid Lie, E. Sheridan, M.-B. Hägg, Energy Procedia 1 (2009) 261.
[11] S.K. Schnell, X. Liu, J.-M. Simon, A. Bardow, D. Bedeaux, T.J.H. Vlugt, S. Kjelstrup, J. Phys. Chem. B 115 (2011) 10911.
[12] S.K. Schnell, T.J.H. Vlugt, J.-M. Simon, D. Bedeaux, S. Kjelstrup, Chem. Phys. Lett. 504 (2011) 199.
[13] S.K. Schnell, T.J.H. Vlugt, J.-M. Simon, D. Bedeaux, S. Kjelstrup, Mol. Phys. 110 (2011) 1069.
[14] J.W. Gibbs, The Scientific Papers of JW Gibbs, vol. 1, Dover, New York, 1961.
[15] J.W. Gibbs, On the Equilibrium of Heterogeneous Substances, Connecticut Academy of Arts and Sciences, 1877.
[16] T.T. Trinh, T.J. Vlugt, M.B. Hagg, D. Bedeaux, S. Kjelstrup, Front. Chem. 1 (2013) 38.
[17] T.S. van Erp, T.T. Trinh, S. Kjelstrup, K. Glavatskiy, Front. Phys. 1 (2013) 30.
[18] J.J. Potoff, J.I. Siepmann, AIChE J. 47 (2001) 1676.
[19] M.P. Allen, D.J. Tildesley, Computer Simulation of Liquids, Oxford University Press, 1989.
[20] S. Plimpton, P. Crozier, A. Thompson, LAMMPS – Large-scale Atomic/Molecular Massively Parallel Simulator, Sandia National Laboratories, 2007.
[21] G.J. Martyna, M.L. Klein, M. Tuckerman, J. Chem. Phys. 97 (1992) 2635.
[22] J. Cox, D.D. Wagman, V.A. Medvedev, CODATA Key Values for Thermodynamics, Chem/Mats-Sci/E, 1989.